Available online at www.sciencedirect.com
ScienceDirect
Journal of the European Ceramic Society 29 (2009) 1521–1528
www.elsevier.com/locate/jeurceramsoc

Quantitative model for the viscous flow and composition of two-phase silicon nitride-based particles in plasma-spray deposition

Y. Bao [a], T. Zhang [b,*], D.T. Gawne [a], P. Mason [b]

[a] *Department of Engineering Systems, London South Bank University, London SE1 0AA, UK*
[b] *Faculty of Engineering, Kingston University, London SW15 3DW, UK*

Received 23 June 2008; received in revised form 22 September 2008; accepted 24 September 2008
Available online 18 November 2008

Abstract

Silicon nitride does not melt but decomposes at 1900 °C and so thermal spraying of pure silicon nitride powder is impracticable. However, the use of silicon nitride and other non-oxide ceramics as thick, thermally sprayed coatings has considerable engineering potential owing to their unique combination of properties. This research shows that embedding fine silicon nitride particles within an oxide matrix to form composite feedstock particles enables the formation of silicon nitride composite coatings with little decomposition of the silicon nitride. Successful deposition of the coatings depends critically on the flow of the feedstock particles on impact with the substrate. This paper concerns the design of oxide matrix systems for the deposition of silicon nitride composite coatings by thermal spraying. A quantitative model is developed for the viscous flow of two-phase feedstock particles at impact. A number of matrix systems are investigated, including a series of yttria–alumina and yttria–alumina–silica compositions. The research shows that certain oxide matrices can provide the required viscous flow and protect the silicon nitride from decomposition.

Keywords: Thermal spray; Silicon nitride; Ceramic coatings; Ceramic processing

1. Introduction

Non-oxide ceramics, such as silicon nitride, silicon carbide, tungsten carbide and aluminum nitride, have a unique combination of high strength, high toughness, wear resistance and thermal and chemical stability. There has been a considerable interest in the use of these materials as monolithic components in industrial applications such as ball and roller bearings, valves in internal combustion engines and cutting tool bits. However, their application is severely limited by their brittleness and poor formability. Using the ceramics as surface coatings rather than bulk materials has major potential in overcoming these weaknesses. The substrate can be selected to provide formability and fracture toughness, while giving support to the essentially brittle coating and enabling it to impart the required surface properties. Furthermore, the coating of machined or formed metal components is often a much cheaper manufacturing route than the sintering of monolithic ceramic components, particularly for medium and large sizes. However, there is no industrial process for producing thick coatings of non-oxide ceramics.

Non-oxide ceramics can be deposited by chemical and physical vapour deposition but the deposition rates are very slow, the size of the components is limited by the coating chamber and the processes are expensive. Thermal spraying, particularly plasma-spraying, has been very successful in producing thick (0.1–1.0 mm) coatings of oxide ceramics such as alumina, yttria–zirconia and chromia. The process consists of injecting powder feedstock particles into a hot jet in which they melt and impact on the substrate to form a coating. The difficulty with non-oxide particles is that they decompose rather than melt in the jet and so coatings cannot be formed by this method. Nevertheless, work has been carried out aimed at thermally spraying silicon nitride-based coatings by in-flight nitridation of silicon,[1] metallic binders,[2] pre-reacted β′-sialon,[3] and oxide binders.[4] These projects met with varying degrees of success but none have produced adequate coating microstructures or coating properties.

The critical process step in plasma-spray deposition is the impact of a feedstock particle with the substrate and its

* Corresponding author.
E-mail address: t.zhang@kingston.ac.uk (T. Zhang).

0955-2219/$ – see front matter © 2008 Published by Elsevier Ltd.
doi:10.1016/j.jeurceramsoc.2008.09.023

subsequent biaxial flow to form a roughly disc-shaped splat. The order of a million of such impacts occurs per second in conventional spraying and the resulting splats agglomerate to form a coating. Each particle cools at a rate of up to 10^7 K s^{-1} and so the flow needs to be both rapid and extensive in order to make effective contact with the undulations of the underlying substrate topography. Otherwise, voids and a porous coating will be produced. This research involves the preparation of composite feedstock particles in which fine silicon nitride particles were encapsulated in an oxide matrix and then plasma-sprayed to form a coating. The flow of these composite particles is crucial for the successful deposition of dense coatings. The presence of the solid silicon nitride phase as well as the nature of the oxide matrix phase are both likely to influence the flow. A model for the flow of composite particles is developed in this paper and applied to design the composition and volume fraction of matrix phases suitable for plasma deposition.

2. Experimental procedure

The silicon nitride used was a standard α-Si_3N_4 powder (containing 95% α-Si_3N_4 and 4% β-Si_3N_4) with a mean particle size of 1.1 μm from CFI Bayer. The substrate material used was a plain carbon steel. The steel was degreased and grit-blasted by using alumina grit with a pressure-operated machine to give a surface roughness (R_a) of 5–6 μm immediately before spraying. The plasma-spray deposition was carried out using a Sulzer-Metco system with a modified MBN torch and MCN control unit. A Metco 4 MP powder feed unit and fluidised bed hopper were used to feed the powder externally into the plasma jet. The coatings were deposited on the steel substrate using a plasma arc power of 26–30 kW and a plasma gas mixture of argon with 5–7% hydrogen. Wipe testing was carried out in order to observe the flow behaviour of isolated splats. It consists of scanning the plasma torch across the target surface sufficiently rapidly such that the individual splats do not overlap one another on impact with the substrate surface. X-ray diffractometry was used to assess the phase composition of feedstock powders and plasma-deposited coatings. A Philips X'pert MRD Diffractometer was used. The sample was scanned by a nickel filtered Cu Kα radiation with a wavelength of 0.15418 nm at a scan rate of 4 °/min.

The wear behaviour of the coatings was determined using a reciprocating machine with alumina balls (Alsint: Fisher Science, UK) sliding over a flat-coated specimen. The applied load was 10 N, the track length 12 mm, and sliding frequency 60 cycles/min (one cycle is 2 × 12 mm). Wear was assessed using a calibrated linear variable differential transducer to measure wear depth. The adhesion of the coating to substrate was assessed using the pull-off tensile test that conforms to ASTM D4541 and BS 3900-E10. The adhesion measurement is performed on a tensile machine. The crosshead speed (related to strain rate) used in the tests was 5 mm/min. The coating surface was roughened with carbide paper and the test cylinder was grit-blasted before applying the adhesive in order to maximize the strength of the adhesive joint.

3. Results and discussion

3.1. Process model

The relevant unit process in thermal-spray deposition is the flow of a feedstock particle into a splat on impact with the substrate. The flow needs to be extensive in order for the materials to enter and make close contact with the valleys and pores of the underlying splats and substrate. Moreover, because of the rapid solidification of the splats after impact, this flow has to take place in a very short time. As a result, both the rate of flow (or strain rate) and the extent of flow are essential parameters to provide bonding and minimize void formation. The model developed below is aimed at providing an insight into the factors governing this fundamental mechanism in the deposition process.

Assuming that a feedstock particle undergoes viscous flow on impact with the substrate according to simple Newtonian behaviour:

$$\tau = \eta \frac{\partial U_x}{\partial Y} \tag{1}$$

where τ is the shear stress, η the viscosity, U_x the velocity in the direction parallel to the surface of the substrate, and y the dimension perpendicular to the surface. Eq. (1) can be written:

$$\tau = \eta \frac{\partial}{\partial y}\left(\frac{\partial x}{\partial t}\right) = \eta \frac{\partial}{\partial t}\left(\frac{\partial x}{\partial y}\right) \tag{2}$$

$$\tau \sim \eta \left(\frac{\Delta x/\Delta y}{\Delta t}\right) \tag{3}$$

In the case of thermal spray deposition, Δy can be taken as the initial diameter of the particle, Δx the diameter of the splat and $\Delta x/\Delta y$ the strain ε. Eq. (3) then may be written:

$$\tau = \eta\varepsilon/\Delta t \tag{4}$$

$$\tau = \eta\varepsilon' \tag{5}$$

where ε' is the strain rate.

It is more convenient in thermal spray deposition to deal with a normal impact stress σ rather than a shear stress τ. σ can be related to the maximum value of the shear stress by:

$$\tau = \frac{\sigma}{2} \tag{6}$$

Ref. [5] gives the stress generated by the impact of feedstock particles of density ρ and velocity u as:

$$\sigma = \frac{\rho u^2}{2} \tag{7}$$

Combining Eqs. (5)–(7) yields:

$$\varepsilon' = \frac{\rho u^2}{4\eta} \tag{8}$$

Eq. (8) indicates that the strain rate of an impacting particle, for a given process condition, is related to the viscosity of the material. The desirable high strain rates, therefore, require low viscosities.

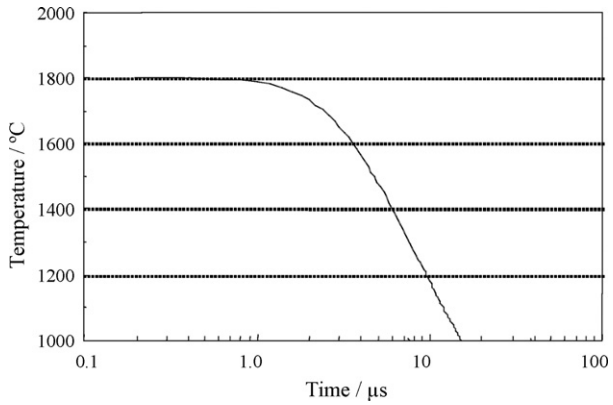

Fig. 1. Calculated cooling curves showing the variation of the average temperature of a 10 μm-thick silicon nitride splat on a steel substrate.

The strain of impacting particles can be obtained from the aspect ratio of splats measured from cross-sections through thermally sprayed coatings and the particle size. For example, measurements on plasma-sprayed alumina coatings gave an average true strain of approximately 2.5. Plasma-spraying can provide particles with high velocities (e.g., ~200 ms^{-1}) and therefore high impact stress but the time available for adequate particle flow before freezing is short and so high strain rates are required. Achieving a high strain rate while avoiding the decomposition of the silicon nitride particle is, therefore, the key to successful deposition.

Fig. 1 gives a computed cooling curve (using the analysis given in Ref. [6]) for a 10 μm-thick silicon nitride splat on a steel substrate. It indicates that the time, Δt, the material spends in the possible viscous temperature range (>1000 °C allowing for undercooling effects) is approximately 20 μs. The strain rate ε' given by $\varepsilon/\Delta t$ is very approximately $10^5\ s^{-1}$. Substituting these values into Eq. (8) and taking a density of 3.3 Mg m^{-3} for sintered silicon nitride yields a required viscosity of very approximately 300 Pa s. If the viscosity is much higher than this value, the desired strain rate is unlikely achieved. Since silicon nitride must remain in the solid state to avoid decomposition, the model indicates that silicon nitride particles cannot flow sufficiently during conventional plasma-spraying to form a coating.

A possible solution is to mix the silicon nitride particles with a matrix phase or binder that does melt in the plasma and form composite feedstock particles. The aim is that the matrix will provide a lubricating function that enables the flow of solid Si_3N_4 particles at high temperatures. The Si_3N_4 particles will clearly need to be substantially smaller than the feedstock particle size. In addition, the matrix phase will need to be strong enough to bind the solid Si_3N_4 particles together after cooling and provide a high-strength coating. From the above model, the viscosity of the composite is a major control factor for the design of a matrix system for the deposition of silicon nitride coatings.

3.2. Important parameters governing the viscosity of the composite

In the melting temperature range of the matrix phase, the composite particles can be considered as a system consisting of liquid and solid phases. The viscosity of such a system may be expressed as:[7–9]

$$\eta = \eta_o \left[1 + 0.75 \frac{V/V_m}{1 - (V/V_m)}\right]^2 \tag{9}$$

or

$$\eta = \eta_o \left[\frac{V_m - 0.25\,V}{V_m - V}\right]^2 \tag{10}$$

where V_m is the maximum volume loading of solid particles. V is the actual volume fraction of solid particles within composite. η_o is the viscosity of the liquid phase. The above equations indicate that the viscosity of the composite is proportional to the viscosity of the liquid phase and also affected by the volume fraction of solid phase. The η_o and V are therefore two important parameters controlling the viscosity of a silicon nitride–matrix system and hence the flow behaviour of the composite particles during thermal spray deposition.

The viscosity, η, of the system can be expressed as a relative viscosity η_r, so that equation (10) becomes:

$$\eta_r = \frac{\eta}{\eta_o} = \left[\frac{V_m - 0.25V}{V_m - V}\right]^2 \tag{11}$$

For a given matrix material and V_m, η_r is a function of the volume fraction of the solid phase. The factor $(V_m - V)$ represents how much the particle volume fraction is short of the maximum particle loading. The free volume remaining at maximum packing, $(1 - V_m)$, relates to the interstices between the contacting solid particles. This volume is required to be filled by the liquid phase. Eq. (11) shows that the viscosity approaches infinity as the volume loading of solid increases to V_m.

A difficulty with Eq. (11) is the uncertainty in the value of V_m as there is no accurate analytical route to its prediction from knowledge of the particle size distribution, particle shape and specific surface area. However, V_m is related to the particle size of the solid phase. V_m decreases with reducing particle size, particularly with sub-micron size particles. The work of Zhang and Evans[9] indicated that V_m values between 0.65 and 0.75 were possible in ceramic injection moulding. These V_m values were used in Eq. (11) to calculate relative viscosities and the results are given in Fig. 2. The results show that the viscosity increases rapidly when the particle content approaches the maximum packing fraction. Furthermore, the viscosity at high particle loadings is very sensitive to the maximum packing density. Although the conditions of flow in thermal spraying differ from those of injection moulding (strain rates of $10^5\ s^{-1}$ compared with 10^2 to $10^3\ s^{-1}$ and temperatures of approximately 1600 °C compared with approximately 200 °C), the physical mechanism is similar and the above model provides a useful basis for understanding the effect of solid fraction on impact flow. Eqs. (9)–(11) suggest that for a given matrix system there is a limitation for the volume loading of silicon nitride within a composite particle.

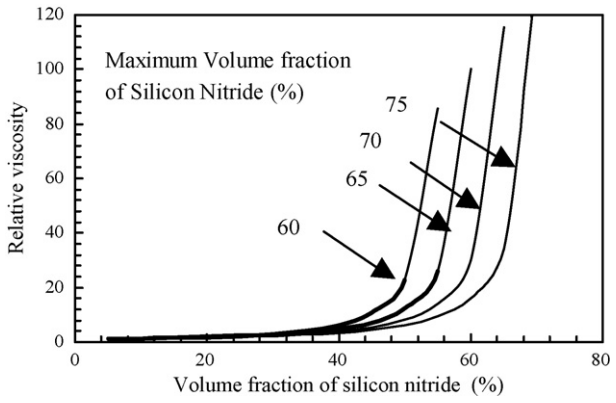

Fig. 2. Calculated relative viscosities (η_r) with respect to maximum packing fraction (V_m) and actual particle fraction (V).

3.3. Materials systems for the matrix phase

In addition to the above viscosity considerations, the selection of a matrix system also depends upon: (a) chemical stability in the high-temperature plasma jet; (b) compatibility with silicon nitride; (c) mechanical strength for the final coating properties.

Oxides are well known to be stable under the conditions of thermal spraying, including atmospheric plasma-spraying, and satisfy criterion (a). Silicon nitride particles are usually covered with a thin layer of silica and so an oxide matrix is likely to be able to bond with silicon nitride [criterion (b)]. Silicon nitride decomposes at approximately 1900 °C and oxides melting below this temperature would appear to be advantageous. A matrix material with a low melting temperature would also benefit feedstock powder preparation and possibly splat flow.

3.3.1. Si_3N_4–YAS system

The system Y_2O_3–Al_2O_3–SiO_2 (denoted YAS) was first chosen since it meets the fundamental criteria. The ternary phase diagram for the Y_2O_3–Al_2O_3–SiO_2 system is given in Fig. 3 [10] and shows a eutectic with a melting temperature of ~1400 °C at a composition of 40 wt% of Y_2O_3, 25 wt% Al_2O_3 and 35 wt% SiO_2 (YAS). This temperature is much lower than that for the decomposition of silicon nitride (~1900 °C). In addition, Y_2O_3 and Al_2O_3 are widely used as sintering additives for silicon nitride and so they are expected to be compatible.

A simple mixture of 40 wt% of Y_2O_3, 25 wt% Al_2O_3 and 35 wt% SiO_2 powders was sintered in air at 1350 °C for 30 min to ensure the formation of required eutectic phase, since there would be insufficient time to produce the equilibrium phases during plasma-spray deposition. The sintered mixture was crushed and ground to the particle size of <75 μm. Wipe tests under plasma-spray were then carried out with the YAS particles on glass slides. The results in Fig. 4 show that significant flow is obtained on impact with the substrate, which indicates that this material is a viable candidate as a matrix phase.

The YAS powder was then mixed with fine silicon nitride powder in a wet ball mill. The slurry was spray dried and the resulting powder was sintered at 1350 °C in a nitrogen atmosphere for 1 h to produce a composite powder consisting of fine silicon nitride particles embedded in YAS matrix. The first composite powder contains 70 vol% silicon nitride. Fig. 5(a) gives the morphologies of impinging particles on a glass slide produced by plasma-spraying using the wipe test. Comparison of the morphologies in Fig. 5(a) with those in Fig. 4 (for pure YAS) shows that the presence of solid silicon nitride particles greatly reduces the flow of YAS. A plasma-sprayed coating produced with this powder gave a poor microstructure with a high porosity. The results fit the predication from Eq. (11). The volume fraction of the silicon nitride was accordingly reduced to from 70 to 60 vol%. The particle flow was improved significantly as shown in Fig. 5(b). Microscopic examination of polished cross-sections of the 60% Si_3N_4–YAS coating revealed improved coating density and uniformity but the porosity of the coatings was still relatively high, particularly at the splat boundaries (Fig. 6). These defects weaken the bonding between splats and also the cohesion strength of the coating. These results suggest that the particle flow of the 60% Si_3N_4–YAS composite powder is still inadequate. From Eq. (11), if a 60 vol% silicon nitride content is to be maintained in the coating, a further reduction in the viscosity of the composite system can only be achieved by reducing the viscosity of the matrix phase η_o.

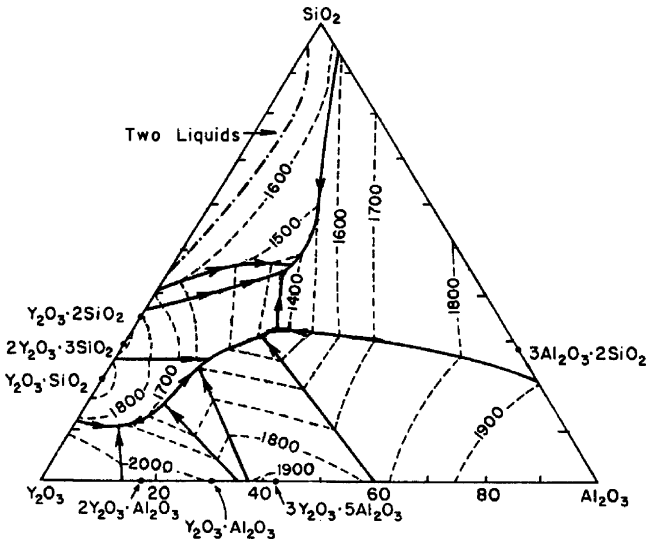

Fig. 3. Ternary phase diagram for the Y_2O_3–Al_2O_3–SiO_2 system[10].

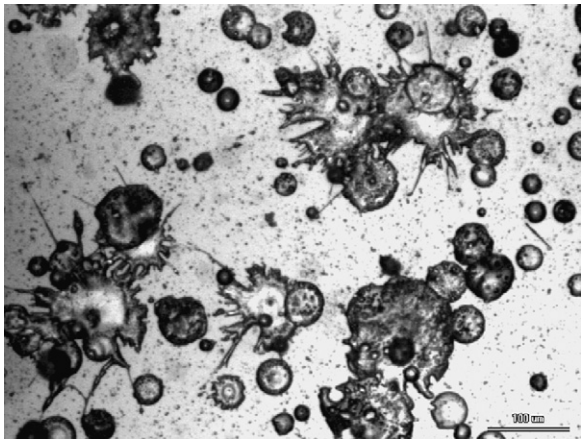

Fig. 4. Morphologies of impinging YAS particles on glass slides produced by wipe test.

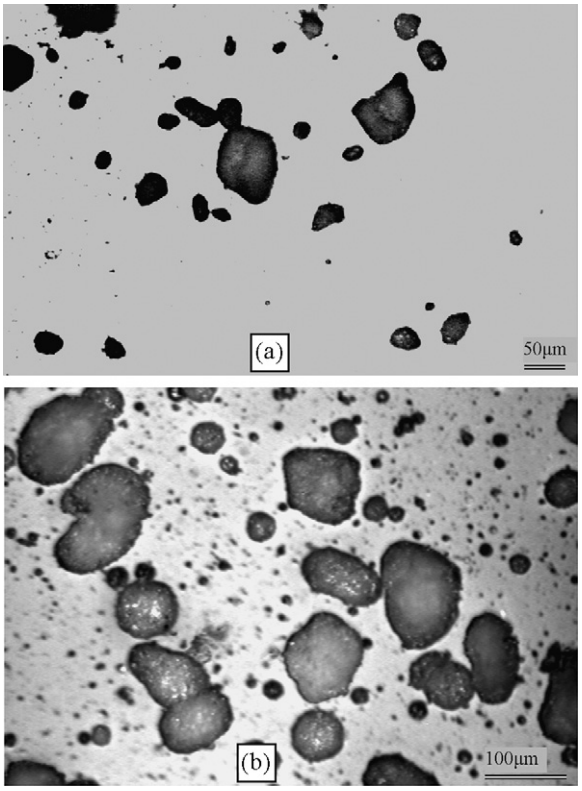

Fig. 5. Morphologies of impinging (Si_3N_4–YAS) composite particles on glass slides produced by wipe testing: (a) 70 vol% Si_3N_4 and (b) 60 vol% Si_3N_4.

Table 1
Viscosities of various glasses at 1500 °C.

	wt% SiO_2	Viscosity (Pa s)
Fused silica	>99.5	2×10^8
Silica glass	96	8×10^6
Borosilicate	81	90
Soda-lime glass	74	30

3.3.2. Si_3N_4–YA system and matrix viscosity

The viscosity of a ceramic melt is determined by its chemical composition and microstructure. Since there are no viscosity data available for the specific materials used here, a consideration of the viscosities of related materials in Table 1 is useful.[11]

The viscosity of glasses is clearly a complex function of composition, particularly in relation to network formers and modifiers, and so Table 1 is an over-simplification. However, silica is a strong network former and its presence will generally increase the viscosity of the melt as suggested in Table 1. The relatively high silica content of YAS is therefore expected to raise its intrinsic viscosity η_o, and hence will increase the viscosity of the Si_3N_4–YAS suspension. The use of YAS as a matrix phase in the presence of high silicon nitride loadings will therefore restrict the flow of composite particles and this accounts for the limited quality of the Si_3N_4–YAS coatings.

From the ternary phase diagram for the Y_2O_3–Al_2O_3–SiO_2 system, a Y_2O_3–Al_2O_3 system in the form of $3Y_2O_3{\cdot}5Al_2O_3$ was chosen as a matrix system (denoted YA). The YA system contains no silica, which should provide a lower viscosity to the benefit of the splat flow of its composite particles. The YA material in the form of $3Y_2O_3{\cdot}5Al_2O_3$ ($Y_3Al_5O_{12}$) was produced by co-precipitation. Fig. 7 gives an optical micrograph showing the morphologies of $Y_3Al_5O_{12}$ particles produced by wipe testing during plasma-spraying. It shows that extensive particle flow took place on impact with the substrate during plasma-spraying suggesting that YA possesses a lower η_o than that of YAS.

A 60 vol% silicon nitride–YA composite powder was then prepared in the same way as described for the silicon nitride-YAS system. Fig. 8 gives examples of the morphologies of the

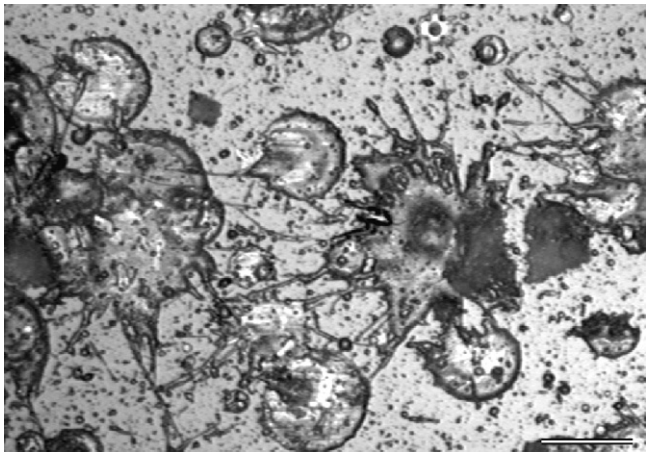

Fig. 7. Splat morphologies showing extensive flow of YA particles on glass slide.

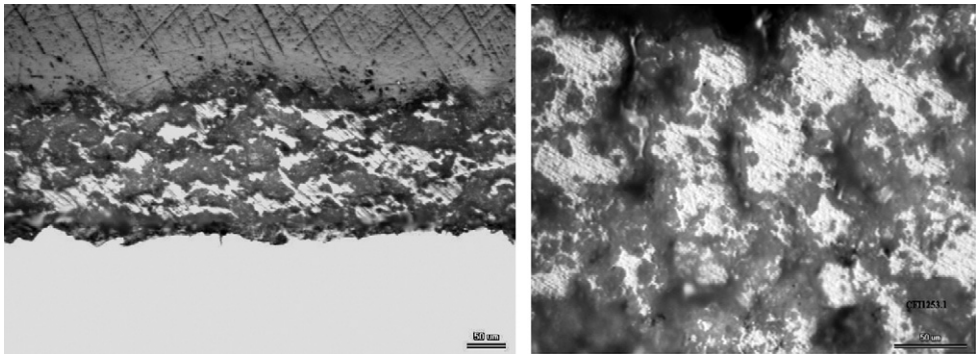

Fig. 6. Polished cross-sections of 60 vol% Si_3N_4–YAS coatings.

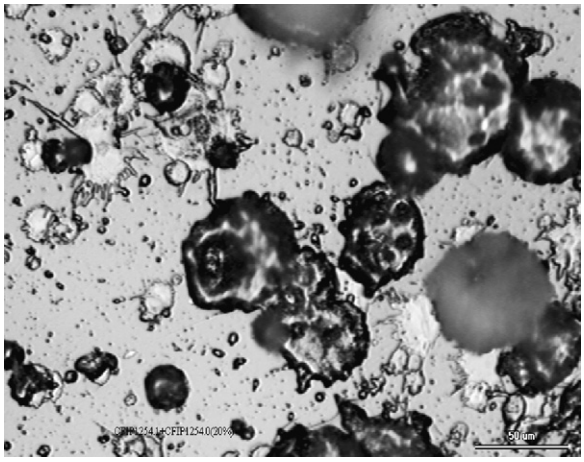

Fig. 8. Splat morphologies of 60 vol% SN–YA particles on glass slide.

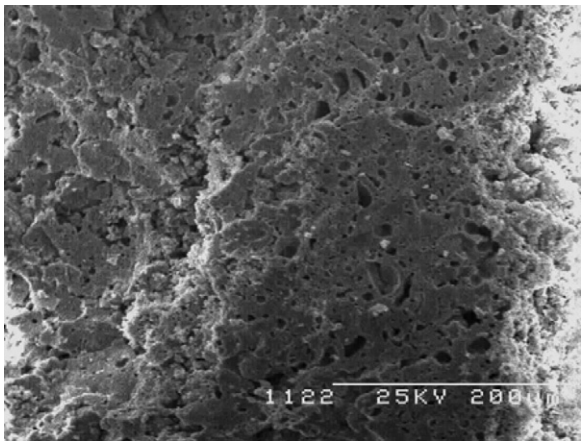

Fig. 10. SEM micrograph showing fracture surface of a 60 vol% SN–YA composite coating.

impinging 60 vol% Si_3N_4–YA particles on glass slides produced by wipe testing under different plasma conditions; it reveals that the majority of the composite particles were able to flow into splats upon impact with the substrate. This implies that most of the Si_3N_4–YA composite particles had formed droplets during their travel through plasma jet and this was caused by the melting of the YA phase. Comparison of the Si_3N_4–YA particle morphologies in Fig. 8 with those of the silicon nitride–YAS particles in Fig. 5 indicates that a significant improvement in particle flow has been achieved by using the YA matrix phase. It was noted that increasing the plasma arc power raised the percentage of well-formed splats and the degree of splat flow. This is expected to produce denser coatings. However, it was also noted that the coatings produced using high arc power contained a high percentage of large pores, suggesting that a high plasma arc power may have resulted in decomposition. In addition, the percentage of pores was found to increase significantly at slow plasma torch traverse speeds, under which conditions excessive thermal energy would have been applied per unit time to the coating material. These results suggest that there is a thermal window for deposition: the particle temperature needs to be high enough for adequate splat flow but not too high to cause decomposition of the materials.

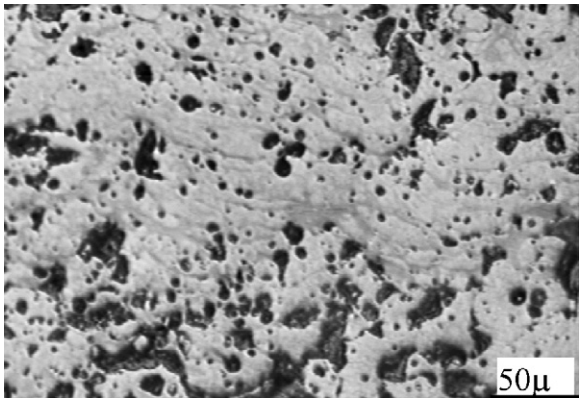

Fig. 9. Optical micrograph showing a polished cross-section of a 60 vol% SN–YA composite coating.

Fig. 9 gives an optical micrograph showing the polished cross-section of a plasma-sprayed 60 vol% Si_3N_4–YA composite coating. Fig. 10 is an SEM micrograph showing fracture surface of a 60 vol% Si_3N_4–YA composite coating. Microscopic examination revealed that the Si_3N_4–YA coatings appear much denser than the Si_3N_4–YAS coatings due to improved particle flow.

3.4. Phase characteristics

The X-ray diffraction spectra from the pure silicon nitride powder, the sintered Si_3N_4–40 wt% YAS composite powder and the plasma-sprayed (Si_3N_4–40 wt% YAS) coating are given in Fig. 11. The data shows that the α-silicon nitride phase is still present in the composite powder after sintering and also in the coating after spraying. The results show that the decomposition of silicon nitride has been prevented by encapsulation in the YAS matrix. There are none of the peaks expected from the possible crystalline phases in the Y_2O_3–Al_2O_3–SiO_2 system, suggesting a glassy phase YAS is formed in the coating.

YAS plays an important role in deposition. It melts at the comparatively low temperature of 1400 °C. The silicon nitride particles become encapsulated in molten YAS during their flight in the plasma and this protects them from decomposition. On impact with the substrate, however, the above results show that the rapid cooling produces a glassy phase with no distinct solidification and an increasingly high melt-viscosity with falling temperature.

The melting temperature of $3Y_2O_3{\cdot}5Al_2O_3$ is 1970 °C, which is higher than the decomposition temperature of silicon nitride (∼1900 °C). There is therefore a danger that it may not protect silicon nitride from decomposition in the plasma jet. Fig. 12 gives the X-ray diffraction spectra of the 60% Si_3N_4–YA powder and coatings deposited under various plasma arc conditions. The data reveal that all the α-Si_3N_4 peaks detected in the powder remain in the X-ray spectra of the plasma-sprayed Si_3N_4–YA coatings, although the intensity appears slightly reduced. This suggests that there is no α-Si_3N_4 to β-Si_3N_4 phase transition during deposition and the main Si_3N_4 phase of the coating

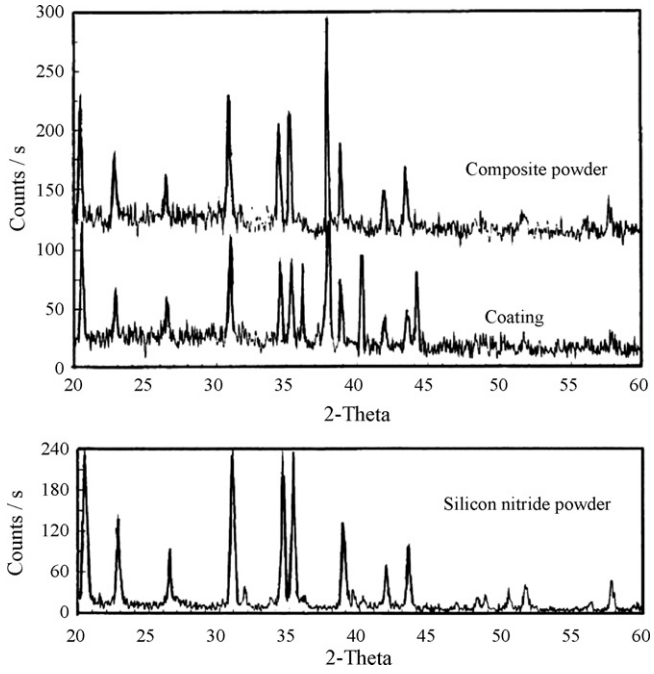

Fig. 11. X-ray diffraction spectra from pure Si_3N_4 powder, the 60 vol% Si_3N_4–YAS composite powder and plasma-sprayed 60 vol% Si_3N_4–YAS composite coating.

is α-Si_3N_4. The reduced intensity may be related to factors such as a variation of the coating composition after spraying, or possibly some degree of silicon nitride decomposition. The X-ray diffratometry analysis also reveals that the $Y_3Al_5O_{12}$-related peaks detected in the powder have all substantially reduced in the coatings. This suggests a tendency for the crystalline phases of $Y_3Al_5O_{12}$ to change into a glassy phase during deposition due to the fast cooling rate of the plasma-spraying process.

A heat transfer calculation using a theoretical method developed by the authors[12] was carried out to estimate the influence of the additives on the temperature profile of in-flight composite particles. Fig. 13 shows the effect of an addition of a secondary phase (melting temperature T_m of 1600 °C, thermal conductivity of 6 W/K m) to the heating of the silicon nitride-based composite particles. The composite particle absorbs additional heat due to the enthalpy of melting of the secondary phase and so the temperature rise within the melting range of the secondary phase

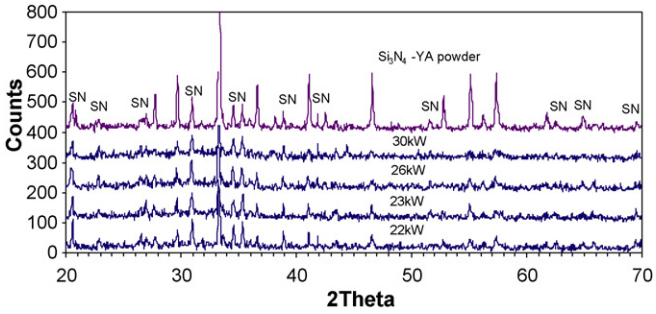

Fig. 12. XRD trace of Si_3N_4–YA powders and coatings sprayed under different arc powers.

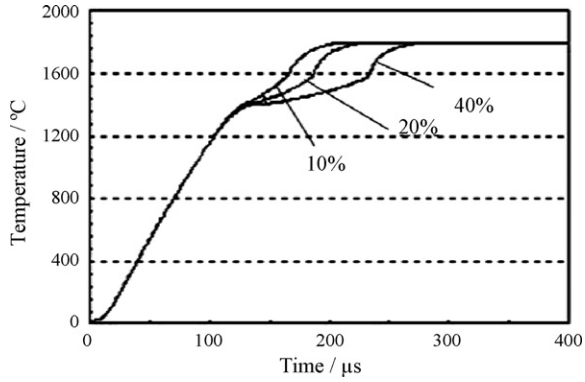

Fig. 13. The influence of secondary phase on the calculated average temperature of a 40 μm silicon nitride composite particle.

is much slower than that of pure silicon nitride. This has the beneficial effect of delaying the decomposition of silicon nitride (decomposition temperature T_{dc}). During cooling of the particle as it impacts on to the substrate, heat will be evolved from the solidification enthalpy, which has the further beneficial effect of extending the residence time in the temperature range of the viscous flow.

3.5. Coating properties

The reciprocating sliding wear testing against an alumina ball was carried out on silicon nitride–YA composite coatings sprayed with 45–63 μm, 38–63 μm and <38 μm 60 vol% Si_3N_4–YA composite powders. The load applied was 10 N. The measured wear rate in the equilibrium stage for those coatings are 2.0 nm/cycle for <38 μm powder, 3.0 nm/cycle for the 38–45 μm powder and 3.2 nm/cycle for the 45–63 μm powder. The results showed that classification to reduce the particle size significantly improved the coating quality. Optical microscopy of the alumina ball counterface used in the wear test revealed that it had been worn severely due to sliding against the SN–YA coatings (Fig. 14), which reflects the high hardness of the sprayed coatings.

Fig. 14. Optical micrograph showing the worn surface of a alumina ball after sliding against a Si_3N_4–YA coating.

The density of the 60 vol% silicon nitride–YA composite coating was measured on the coating detached from substrate using Archimedes' principle. It was found that the average density of the coating was 3.42 g/cm^3. The calculated theoretical density of the composite coating is 3.56 g/cm^3 and so the relative density of the coating is 96%. It should be mentioned that during the measurement the coatings were immersed in water and the water may penetrate into open pores. The open pores of the coating could therefore not to be taken into account for the calculation of the coating density and this may cause errors in the experimental results. The Vickers hardnesses of the coatings were determined with a Mitutoyu hardness tester using a 50 g load for 15 s (avoiding the apparent porous areas of the coatings). The average measured hardness was 1260 HV50.

4. Conclusions

1. A quantitative model is presented for the viscous flow of two-phase feedstock particles on impact with the substrate. The model has been applied to the design of matrix systems for silicon nitride composite coatings.
2. The critical requirement of the viscous flow of the composite particles is governed by the viscosity of the oxide matrix phase and the volume fraction of the silicon nitride particles. High silicon nitride loadings are shown to result in very large increases in the viscosity, inadequate splat flow and poor coating structures
3. Si_3N_4–YAS coatings have been developed in which the low melting point YAS matrix phase successfully protects the silicon nitride from decomposition. However, the quality of these coatings is limited by their relatively high silica content of the YAS, which adversely affects the particle flow on impact.
4. The coatings produced by using YA (Y_2O_3–Al_2O_3) as a matrix phase have higher density and wear resistance than those produced by using the YAS (Y_2O_3–Al_2O_3–SiO_2) phase. This is due to the lower viscosity of YA and improved particle flow.
5. The model of deposition is consistent with the experimental observations and provides a basis for the future development of composite coatings.
6. Dense silicon nitride-based composite coatings can be produced without decomposition by selection of a suitable oxide matrix phase.

Acknowledgements

The authors would like to thank the Directorate-General for Science Research and Development of the European Commission for supporting the research and CFI Bayer for their collaboration in the project.

References

1. Eckardt, T., Mallener, W. and Stover, D., Reactive plasma sintering of silicon in controlled nitrogen atmosphere. In *Thermal spray industrial applications*, ed. C. C. Berndt and S. Sampath. ASM International, Materials Park, OH, USA, 1994, pp. 515–519.
2. Lugscheider, E., Limbach, R., Liden, A. and Lodin, Plasma spraying of silicon nitride. *High Temp. Mater. Powder Eng.*, 1990(Part 1), 877–880.
3. Sodeoka, S., Ueno, K., Hagiwara, Y. and Kose, S., Structure and properties of plasma-sprayed sialon coatings. *J. Thermal Spray Technol.*, 1992, **1**, 153–159.
4. Berger, L. M., Herrmaun, M., Nebelung, M., Thiele, S., Heimann, R. B., Schnick, T., Wielage, B. and Vuoristo, P., In *Thermal spray: meeting the challenge of the 21st century*, ed. C. Coddet. ASM International, Materials Park, OH, USA, 1998, pp. 1149–1154.
5. Riney, T. D., Numerical evaluation of hypervelocity impact phenomena. In *High-velocity impact phenomenology*, ed. Kinslow Ray. Academic Press, London, 1970, pp. 157–212.
6. Zhang, T., Gawne, D. T. and Liu, B., Computer modelling of the influence of process parameters on the heating and acceleration of particles during plasma spraying. *Surf. Coat. Technol.*, 2000, **132**, 233–243.
7. Edirisinghe, M. J. and Evans, J. R. G., The rheology of ceramic injection molding blends. *Br. Ceram. Trans. J.*, 1987, **86**, 18–22.
8. Chong, J. S., Christiansen, E. B. and Baer, A. D., Rheology of concentrated suspension. *J. Appl. Polym. Sci.*, 1971, **15**, 2007–2021.
9. Zhang, T. and Evans, J. R. G., Predicting the viscosity of ceramic injection molding suspensions. *J. Eur. Ceram. Soc.*, 1989, **5**, 165–172.
10. Park, D.-S., Kim, H.-D., Lim, K. T., Bang, K.-S. and Park, C., Microstructure of reaction-bonded silicon nitride fabricated under static nitrogen pressure. *Mater. Sci. Eng. A*, 2005, **405**, 158–162.
11. Shand, E. B., *Engineering glasses, modern materials*. Academic Press, New York, 1968, p. 262.
12. Bao, Y., Gawne, D. T. and Zhang, T., The effect of feedstock particle size on the heat transfer rates and properties of thermally sprayed polymer coatings. *Trans. Inst. Metal Finishing*, 1995, **73**(4), 119–124.